Nonforward parton densities and soft mechanism for form factors and wide-angle Compton scattering in QCD

A. V. Radyushkin*
Department of Physics, Old Dominion University, Norfolk, Virginia 23529
and Jefferson Lab, Newport News, Virginia 23606
(Received 28 April 1998; published 28 October 1998)

We argue that, at a moderately large momentum transfer $-t \lesssim 10$ GeV^2, hadronic form factors and wide-angle Compton scattering amplitudes are dominated by a mechanism corresponding to the overlap of soft wave functions. We show that the soft contribution in both cases can be described in terms of the same universal nonforward parton densities (ND's) $\mathcal{F}(x;t)$, which are the simplest hybrids of the usual parton densities and hadronic form factors. We propose a simple model for ND's possessing required reduction properties. Our model easily reproduces the observed magnitude and the dipole t dependence of the proton form factor $F_1^p(t)$ in the region 1 GeV$^2 < -t < 10$ GeV^2. Our results for the wide-angle Compton scattering cross section follow the angular dependence of existing data and are rather close to the data in magnitude. [S0556-2821(98)01321-6]

PACS number(s): 13.60.Fz, 12.38.Bx, 13.60.Le

I. INTRODUCTION

Compton scattering in its various versions provides a unique tool for studying hadronic structure. The Compton amplitude probes the hadrons through a coupling of two electromagnetic currents and in this aspect it can be considered as a generalization of hadronic form factors. In QCD, the photons interact with the quarks of a hadron through a vertex which, in the lowest approximation, has a pointlike structure. However, in the soft regime, strong interactions produce large corrections uncalculable within the perturbative QCD framework. To take advantage of the basic pointlike structure of the photon-quark coupling and the asymptotic freedom feature of QCD, one should choose a specific kinematics in which the behavior of the relevant amplitude is dominated by short (or, more precisely, lightlike) distances. The general feature of all such types of kinematics is the presence of a large momentum transfer. For Compton amplitudes [see Fig. 1(a)], there are several situations when large momentum transfer induces dominance of configurations involving lightlike distances: (i) both photons are far off-shell and have equal spacelike virtuality: virtual forward Compton amplitude, its imaginary part determines structure functions of deep inelastic scattering (DIS); (ii) initial photon is highly virtual, the final one is real and the momentum transfer to the hadron is small: deeply virtual Compton scattering (DVCS) amplitude; (iii) both photons are real but the momentum transfer is large: wide-angle Compton scattering (WACS) amplitude, the study of which is the ultimate goal of the present paper.

Our main statement is that at accessible momentum transfers $|t| \lesssim 10$ GeV^2, the WACS amplitude is dominated by handbag diagrams [Figs. 1(b),1(c)], just like in DIS and DVCS. In the most general case, the nonperturbative part of the handbag contribution is described by nonforward double distributions (DD's) $F(x,y;t), G(x,y;t)$, etc., which can be related to the usual parton densities $f(x)$, $\Delta f(x)$ and nucleon form factors such as $F_1(t), G_A(t)$. Among the arguments of DD's, x is the fraction of the initial hadron momentum carried by the active parton and y is the fraction of the momentum transfer r. The description of the WACS amplitude simplifies when one can neglect the y dependence of the hard part and integrate out the y dependence of the double distributions. In that case, the long-distance dynamics is described by nonforward parton densities (ND's) $\mathcal{F}(x;t), \mathcal{G}(x;t)$, etc. The latter can be interpreted as the usual parton densities $f(x)$ supplemented by a form factor type t dependence. We propose a simple model for the relevant ND's which both satisfies the relation between $\mathcal{F}(x;t)$ and usual parton densities $f(x)$ and produces a good description of the $F_1(t)$ form factor up to $t \sim -10$ GeV^2. We use this model to calculate the WACS amplitude and obtain results which are rather close to existing data.

II. VIRTUAL COMPTON AMPLITUDES

The forward virtual Compton amplitude whose imaginary part gives structure functions of deep inelastic scattering (see, e.g., Ref. [1]) is the classic example of a light cone dominated Compton amplitude. In this case, the ''final'' photon has momentum $q' = q$ coinciding with that of the initial one. The momenta p, p' of the initial and final hadrons also coincide. The total c.m. energy of the photon-hadron system $s = (p+q)^2$ should be above the resonance region, and the Bjorken ratio $x_{Bj} = Q^2/2(pq)$ is finite. The light cone dominance is secured by high virtuality of the photons: $-q^2 \equiv Q^2 \gtrsim 1$ GeV^2. In the large-Q^2 limit, the leading contribution in the lowest α_s order is given by handbag diagrams in which the perturbatively calculable hard quark propagator is convoluted with parton distribution functions $f_a(x)$ $(a = u,d,s,\ldots)$ which describe and parametrize nonperturbative information about the hadronic structure.

The condition that both photons are highly virtual may be relaxed by taking a real photon in the final state. Keeping the momentum transfer $t \equiv (p-p')^2$ to the hadron as small as possible, one arrives at kinematics of the deeply virtual

*Also at Laboratory of Theoretical Physics, JINR, Dubna, Russian Federation.

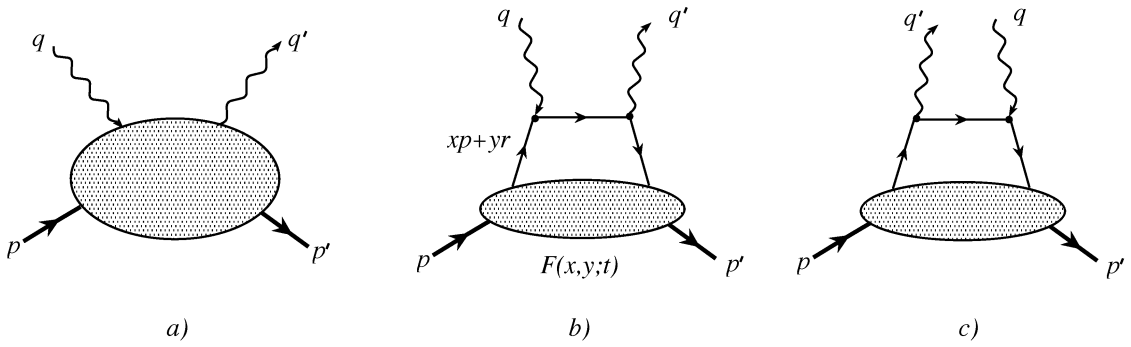

FIG. 1. (a) General Compton amplitude, (b) *s*-channel handbag diagram, and (c) *u*-channel handbag diagram.

Compton scattering the importance of which was recently emphasized by Ji [2] (see also Ref. [3]). Having large virtuality Q^2 of the initial photon is sufficient to guarantee that in the Bjorken limit the leading power contributions in $1/Q^2$ are generated by the strongest light cone singularities [4–7], with the handbag diagrams being the starting point of the α_s expansion. The most important contribution to the DVCS amplitude is given by a convolution of a hard quark propagator and a nonperturbative function describing long-distance dynamics, which in the most general case is given by nonforward double distributions $F(x,y;t), G(x,y;t), \ldots$ [3,5].

The DD's are rather complicated functions. They specify the fractions xp and yr of the initial hadron momentum p and the momentum transfer $r \equiv p - p'$ carried by the active parton: $k \sim xp + yr$. The DD's vanish outside the triangle region $0 \leqslant x+y \leqslant 1$ [3,5]. In addition to x and y, they also depend on the invariant momentum transfer $t=(p'-p)^2$. In some limiting cases, the double distributions reduce to simpler and already known functions. For $r=0$, the matrix elements coincide with the forward ones defining the usual parton densities. This results in the following ''reduction relations'' [3,5]:

$$\int_0^{1-x} F^a(x,y;t=0)\,dy = f_a(x). \tag{1}$$

Integrating properly weighted sums of quark and antiquark DD's over x one obtains the Dirac form factor

$$\sum_a e_a \int_0^1 dx \int_0^{1-x} [F^a(x,y;t) - \bar{F^a}(x,y;t)]\,dy = F_1(t), \tag{2}$$

where e_a is the electric charge of the ''a'' quark. Just like for form factors, one should take into account extra double distributions $K^a(x,y;t)$ corresponding to a hadron helicity flip in the nonforward matrix element [2]. These distributions are related to the Pauli form factor $F_2(t)$: one should just substitute $F^{a,\bar{a}}$ by $K^{a,\bar{a}}$ and F_1 by F_2 in Eq. (2). A common element of these reduction formulas is an integration over y. Hence, it is convenient to introduce intermediate functions

$$\mathcal{F}^a(x;t) = \int_0^{1-x} F^a(x,y;t)\,dy,$$

$$\mathcal{K}^a(x;t) = \int_0^{1-x} K^a(x,y;t)\,dy. \tag{3}$$

They satisfy the reduction formulas

$$\mathcal{F}^a(x;t=0) = f_a(x),$$

$$\sum_a e_a \int_0^1 [\mathcal{F}^a(x;t) - \bar{\mathcal{F}^a}(x;t)]\,dx = F_1(t), \tag{4}$$

$$\sum_a e_a \int_0^1 [\mathcal{K}^a(x;t) - \bar{\mathcal{K}^a}(x;t)]\,dx = F_2(t), \tag{5}$$

which show that these functions are the simplest hybrids of the usual parton densities and form factors. For this reason, we call them *nonforward parton densities*. Note that the $t=0$ limit of the ''magnetic'' ND's exists: $\mathcal{K}^a(x;t=0) \equiv k_a(x)$. In particular, the integral

$$\sum_a e_a \int_0^1 [k_a(x) - k_{\bar{a}}(x)]\,dx = \kappa_p \tag{6}$$

gives the anomalous magnetic moment of the proton. Knowledge of the x moment of $k_a(x)$'s is needed to determine the contribution of the quark orbital angular momentum to the proton spin [2]. Since the K-type DD's are always accompanied by the $r_\mu = p_\mu - p'_\mu$ factor, they are invisible in deep inelastic scattering and other inclusive processes related to strictly forward $r=0$ matrix elements.

There are also parton-helicity sensitive double distributions $G^a(x,y;t)$ and $P^a(x,y;t)$. The first one reduces to the usual spin-dependent densities $\Delta f_a(x)$ in the $r=0$ limit and gives the axial form factor $F_A(t)$ after x,y integration. The second one is related to the pseudoscalar form factor $F_P(t)$.

In the DVCS kinematics, $|t|$ is assumed to be small compared to Q^2, and for this reason the t and m_p^2 dependence of the short-distance amplitude in Refs. [2–5] was neglected.[1] This is equivalent to approximating the active parton mo-

[1]One should not think that such a dependence is necessarily a higher twist effect: the lowest twist contribution has a calculable dependence on t and m_p^2 analogous to the Nachtmann-Georgi-Politzer $O(m_p^2/Q^2)$ target mass corrections in DIS [8,9].

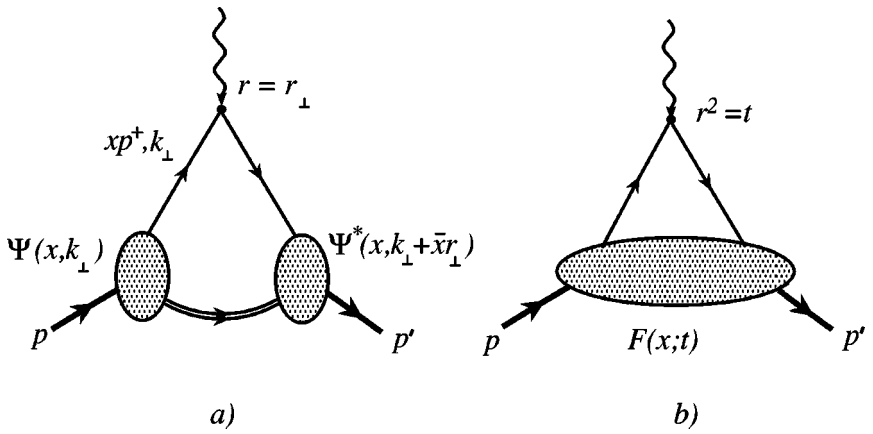

FIG. 2. (a) Structure of the effective two-body contribution to form factor in the light cone formalism. (b) Form factor as an x integral of nonforward parton densities.

mentum k by its plus component alone: $k \to xp^+ + yr^+$. Treating $\zeta \equiv r^+/p^+$ as an external parameter and using the total fraction $X \equiv x + \zeta y$ as an independent variable, one arrives at an alternative description of the DVCS scaling limit in terms of the nonforward parton distributions[2] [10,5] (NFPD's) $\mathcal{F}_\zeta(X;t)$. They are related to double distributions by

$$\mathcal{F}^{a,\bar{a}}_\zeta(X;t) = \int_0^{\min\{X/\zeta, \bar{X}/\bar{\zeta}\}} F^{a,\bar{a}}(X-\zeta y, y; t)\, dy. \qquad (7)$$

In a similar way, one can incorporate the relevant double distributions to define also ''magnetic'' $\mathcal{K}^{a,\bar{a}}_\zeta(X;t)$ and parton-helicity sensitive nonforward distributions $\mathcal{G}^{a,a}_\zeta(X;t)$ and $\mathcal{P}^{a,\bar{a}}_\zeta(X;t)$ [2,14,15]. In addition to the usual parton momentum fraction variable X and the invariant momentum transfer t, the NFPD's also depend on the skewedness parameter $\zeta = r^+/p^+$ specifying the longitudinal momentum asymmetry of the nonforward matrix element. This asymmetry appears because it is impossible to convert a highly virtual initial photon into a real final photon without a longitudinal momentum transfer. In general, one can use different pairs of vectors to specifiy the longitudinal direction: (p,q), (p,q') or (P,q) with $P=(p+p')/2$, etc., resulting in different t-dependent expressions for ζ. However, in the (formal) scaling limit $t \to 0$, $m_p^2 \to 0$ all these expressions for the skewedness parameter ζ coincide with the Bjorken ratio $x_{Bj} = Q^2/2(pq)$ [3,5].

III. MODELING ND'S

Our final goal in the present paper is to get an estimate of the handbag contributions for the large-t real Compton scattering. Since the initial photon in that case is also real: $Q^2 = 0$ (and hence $x_{Bj} = 0$), it is natural to expect that the nonperturbative functions which appear in WACS correspond to the $\zeta = 0$ limit of the nonforward parton distributions[3] $\mathcal{F}^a_\zeta(x;t)$. It is easy to see from Eqs. (3),(7) that in this limit the NFPD's reduce to the nonforward parton densities $\mathcal{F}^a(x;t)$ introduced above:

$$\mathcal{F}^a_{\zeta=0}(x;t) = \mathcal{F}^a(x;t). \qquad (8)$$

The simplification is that ND's depend on ''only two'' variables x and t, with this dependence constrained by reduction formulas (4),(5). Furthermore, it is possible to give an interpretation of nonforward densities in terms of the light-cone wave functions. Consider for simplicity a two-body bound state whose lowest Fock component is described by a light cone wave function $\Psi(x,k_\perp)$. Choosing a frame where the momentum transfer r is purely transverse $r = r_\perp$, we can write the two-body contribution into the form factor [Fig. 2(a)] as [16]

$$F^{(\mathrm{tb})}(t) = \int_0^1 dx \int \Psi^*(x, k_\perp + \bar{x} r_\perp)\Psi(x,k_\perp)\frac{d^2k_\perp}{16\pi^3}, \qquad (9)$$

where $\bar{x} \equiv 1-x$. Comparing this expression with the reduction formula (4), we conclude [see Fig. 2(b)] that

$$\mathcal{F}^{(\mathrm{tb})}(x,t) = \int \Psi^*(x, k_\perp + \bar{x} r_\perp)\Psi(x,k_\perp)\frac{d^2k_\perp}{16\pi^3} \qquad (10)$$

is the two-body contribution into the nonforward parton density $\mathcal{F}(x,t)$. Assuming a Gaussian dependence on the transverse momentum $k_\perp$ (see Ref. [16])

$$\Psi(x,k_\perp) = \Phi(x) e^{-k_\perp^2/2x\bar{x}\lambda^2}, \qquad (11)$$

we get

[2]Other terminology, ''off-forward'' [2], ''nondiagonal'' [11], and ''off-diagonal'' [12,13], is also used in the literature. Off-forward parton distributions introduced by Ji in his pioneering papers on DVCS [2,4] are equivalent though not identical to the nonforward ones, while ''nondiagonal'' and ''off-diagonal'' distributions essentially coincide with NFPD's, see Ref. [5] for details.

[3]Provided that one can neglect the t dependence of the hard part, see a footnote above and discussion in Sec. VI.

$$\mathcal{F}^{(\mathrm{tb})}(x,t)=f^{(tb)}(x)e^{\bar{x}t/4x\lambda^2}, \tag{12}$$

where

$$f^{(\mathrm{tb})}(x)=\frac{x\bar{x}\lambda^2}{16\pi^2}\Phi^2(x)=\mathcal{F}^{(\mathrm{tb})}(x,t=0) \tag{13}$$

is the two-body part of the relevant parton density. Within the light-cone approach, to get the total result for either usual $f(x)$ or nonforward parton densities $\mathcal{F}(x,t)$, one should add the contributions due to higher Fock components. By no means are these contributions small, e.g., the valence $\bar{d}u$ contribution into the normalization of the π^+ form factor at $t=0$ is less than 25% [16]. In the absence of a formalism providing explicit expressions for an infinite tower of light-cone wave functions we choose to treat Eq. (12) as a guide for fixing interplay between the t and x dependences of ND's and propose to model them by

$$\mathcal{F}^a(x,t)=f_a(x)e^{\bar{x}t/4x\lambda^2}=\frac{f_a(x)}{\pi x\bar{x}\lambda^2}\times\int e^{-(k_\perp^2+(k_\perp+\bar{x}r_\perp)^2)/2x\bar{x}\lambda^2}d^2k_\perp . \tag{14}$$

The functions $f_a(x)$ here are the usual parton densities assumed to be taken from existing parametrizations such as Glück-Reya-Vogt (GRV), Martin-Roberts-Stirling (MRS), CTEQ, etc. In the $t=0$ limit (recall that t is negative) this model, by construction, satisfies the first of reduction formulas (4). Within the Gaussian ansatz (14), the basic scale λ specifies the average transverse momentum carried by the quarks. In particular, for valence quarks

$$\langle k_\perp^2\rangle^a=\frac{\lambda^2}{N_a}\int_0^1 x\bar{x}f_a^{\mathrm{val}}(x)dx, \tag{15}$$

where $N_u=2$, $N_d=1$ are the numbers of valence a quarks in the proton.

To fix the magnitude of λ, we use the second reduction formula in (4) relating $\mathcal{F}^a(x,t)$'s to the $F_1(t)$ form factor. To this end, we take the following simple expressions for the valence distributions:

$$f_u^{\mathrm{val}}(x)=1.89x^{-0.4}(1-x)^{3.5}(1+6x), \tag{16}$$

$$f_d^{\mathrm{val}}(x)=0.54x^{-0.6}(1-x)^{4.2}(1+8x). \tag{17}$$

They closely reproduce the relevant curves given by the GRV parametrization [17] at a low normalization point $Q^2\sim 1$ GeV^2. The best agreement between our model

$$F_1^{\mathrm{soft}}(t)=\int_0^1[e_u f_u^{\mathrm{val}}(x)+e_d f_d^{\mathrm{val}}(x)]e^{\bar{x}t/4x\lambda^2}dx \tag{18}$$

and experimental data [18] in the moderately large t region $1\ \mathrm{GeV}^2<|t|<10\ \mathrm{GeV}^2$ is reached for $\lambda^2=0.7$ GeV^2 (see Fig. 3). This value gives a reasonable magnitude

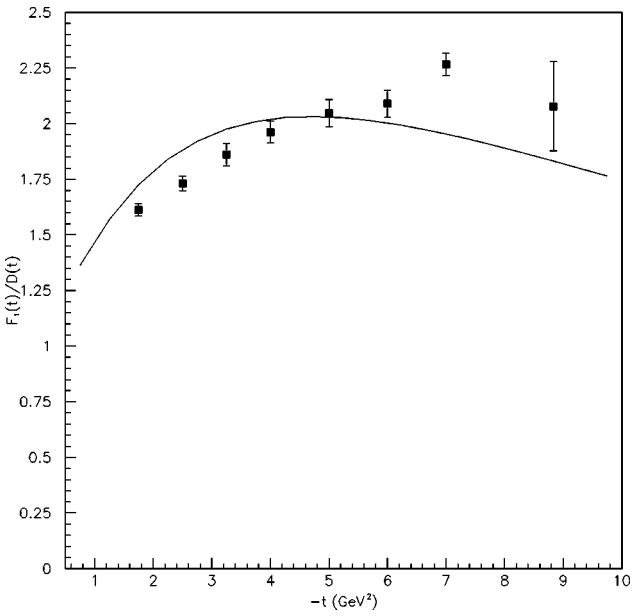

FIG. 3. Ratio $F_1^p(t)/D(t)$ of the $F_1^p(t)$ form factor to the dipole fit $D(t)=1/(1-t/0.71\ \mathrm{GeV}^2)^2$. Curve is based on Eqs. (16)–(18) with $\lambda^2=0.7$ GeV^2. Experimental data are taken from Ref. [18].

$$\langle k_\perp^2\rangle^u=(290\ \mathrm{MeV})^2,\quad \langle k_\perp^2\rangle^d=(250\ \mathrm{MeV})^2 \tag{19}$$

for the average transverse momentum of the valence u and d quarks in the proton.

Similarly, building a model for the parton helicity sensitive ND's $\mathcal{G}^a(x,t)$ one can take their $t=0$ shape from existing parametrizations for spin-dependent parton distributions $\Delta f_a(x)$ and then fix the relevant λ parameter by fitting the $G_A(t)$ form factor. The case of hadron spin-flip distributions $\mathcal{K}^a(x,t)$ and $\mathcal{P}^a(x;t)$ is more complicated since the distributions $k_a(x)$, $p_a(x)$ are unknown.

At $t=0$, our model by construction gives a correct normalization $F_1^p(t=0)=1$ for the form factor. However, if one would try to find the derivative $(d/dt)F_1^p(t)$ at $t=0$ by expanding the exponential $\exp[\bar{x}t/x\lambda^2]$ into the Taylor series under the integral (18), one would get a divergent expression. An analogous problem is well known in applications of QCD sum rules to form factors at small t [19–22]. The divergence is related to the long-distance propagation of massless quarks in the t channel. Formally, this is revealed by singularities starting at $t=0$. However, $F_1^p(t)$ should not have singularities for timelike t up to $4m_\pi^2$, with the ρ-meson peak at $t=m_\rho^2\sim 0.6$ GeV^2 being the most prominent feature of the t-channel spectrum. Technically, the singularities of the original expression are singled out into bilocal correlators [23] which are substituted by their realistic version with correct spectral properties (usually the simplest model with ρ and ρ' terms is used). An important point is that such a modification is needed only when one calculates form factors in the small-t region: for $-t\gtrsim 1$ GeV^2, the correction terms should vanish faster than any power of $1/t$ [21]. In our case, the maximum deviation of the curve for $F_1^p(t)$ given by Eq. (18) from the experimental data in the

small-t region $-t \lesssim 1$ GeV^2 is 15%. Hence, if one is willing to tolerate such an inaccuracy, one can use our model starting with $t=0$.

IV. SOFT VS HARD CONTRIBUTIONS TO FORM FACTORS

Our curve is within 5% from the data points [18] for 1 GeV$^2 \lesssim -t \lesssim 6$ GeV^2 and does not deviate from them by more than 10% up to 9 GeV^2. Modeling the t dependence by a more complicated formula (e.g., assuming a slower decrease at large t and/or choosing different λ's for u and d quarks and/or splitting ND's into several components with different λ's, etc.) or changing the shape of parton densities $f_a(x)$ one can improve the quality of the fit and extend agreement with the data to higher t. Such a fine-tuning is not our goal here. We just want to emphasize that a reasonable description of the $F_1(t)$ data in a wide region 1 GeV$^2 < |t| < 10$ GeV^2 was obtained by fixing just a single parameter λ reflecting the proton size. Moreover, we could fix λ from the requirement that $\langle k_\perp^2 \rangle \sim (300 \text{ MeV})^2$ and present our curve for $F_1(t)$ as a successful prediction of the model. We interpret this success as evidence that the model correctly catches the gross features of the underlying physics.

Since our model implies a Gaussian dependence on the transverse momentum, it includes only what is usually referred to as an overlap of soft wave functions. It completely neglects effects due to hard perturbative QCD (PQCD) gluon exchanges generating the power-law $O[(\alpha_s/\pi)^2/t^2]$ tail of the nonforward densities at large t. It is worth pointing out here that though we take nonforward densities $\mathcal{F}^a(x,t)$ with an exponential dependence on t, the $F_1(t)$ form factor in our model has a power-law asymptotics $F_1^{\text{soft}}(t) \sim (-4\lambda^2/t)^{n+1}$ dictated by the $(1-x)^n$ behavior of the parton densities for x close to 1. This connection arises because the integral (18) over x is dominated at large t by the region $\bar{x} \sim 4\lambda^2/|t|$. In other words, the large-t behavior of $F_1(t)$ in our model is governed by the Feynman mechanism [1]. One should realize, however, that the relevant scale $4\lambda^2 = 2.8$ GeV^2 is rather large. For this reason, when $|t| < 10$ GeV^2, it is premature to rely on asymptotic estimates for the soft contribution. Indeed, with $n=3.5$, the asymptotic estimate is $F_1^{\text{soft}}(t) \sim t^{-4.5}$, in apparent contradiction with the ability of our curve to follow the dipole behavior. The resolution of this paradox is very simple: the maxima of nonforward densities $\mathcal{F}^a(x,t)$ for $|t| \lesssim 10$ GeV^2 are at rather low x values $x \lesssim 0.5$.[4] Hence, the x-integrals producing $F_1^{\text{soft}}(t)$ are not dominated by the $x \sim 1$ region yet and the asymptotic estimates are not applicable: the functional dependence of $F_1^{\text{soft}}(t)$ in our model is much more complicated than a simple power of $1/t$.

The fact that our model closely reproduces the experimentally observed dipole like behavior of the proton form factor is a clear demonstration that such a behavior has nothing to do with the quark counting rules $F_1^p(t) \sim 1/t^2$ [24,25] valid for the asymptotic behavior of the hard gluon exchange contributions. Our explanation of the observed magnitude and the t dependence of $F_1(t)$ by a purely soft contribution is in strong contrast with that of the hard PQCD approach to this problem. Of course, there is no doubt that in the formal asymptotic limit $|t| \to \infty$, the dominant contribution to the $F_1(t)$ form factor in QCD is given by diagrams involving two hard gluon exchanges, with nonperturbative dynamics described by distribution amplitudes (DA's) $\varphi_p(x_1,x_2,x_3)$, $\varphi_p(y_1,y_2,y_3)$ of the initial and final protons [26,27]. However, attempting to describe the data at accessible t by hard contributions only, one is forced to make several unrealistic assumptions.

The crucial element is the use of humpy DA's similar to those proposed by Chernyak and Zhitnitsky [28,27] (CZ). The usual claim is that these DA's are backed by QCD sum rule calculations of their lowest moments. However, as we argued in Ref. [29], a straightforward version of the QCD sum rule approach in this case is unreliable because of poor convergence of the underlying operator product expansion (OPE). In the analysis of the QCD sum rules for the moments of the pion distribution amplitude performed in Refs. [29,30], the contribution of exploding higher terms of the OPE (neglected in the CZ approach) was modeled by nonlocal condensates. The resulting QCD sum rule produces the pion DA close to the asymptotic one. The statement that the pion DA is close to its asymptotic form even at a low normalization point is also supported by a lattice calculation of the second moment of the pion DA [31], by QCD sum rule estimate of the magnitude of $\varphi_\pi(x)$ at the middle point $x=1/2$ [32], by the analysis of QCD sum rules for the nondiagonal correlator [33,34], by calculation of the pion DA in the chiral soliton model [35], and by a direct QCD sum rule calculation of the large-Q^2 behavior of the $\gamma^*\gamma\pi^0$ form factor [36]. Furthermore, within the light-cone QCD sum rule approach one can relate the pion DA to the pion parton densities [37] known experimentally. According to the analysis performed in Ref. [38], existing data favor the asymptotic shape. Finally, the humpy pion DA advocated in Ref. [39,27] is now ruled out by recent experimental data [40] on the $\gamma^*\gamma\pi^0$ form factor. The data are fully consistent with the next-to-leading PQCD prediction calculated using the asymptotic DA [41–43].

Since the structure of OPE in the pion and nucleon cases is very similar, we see no reason to expect a significant deviation of the nucleon DA from its asymptotic form. In particular, evidence against humpy nucleon DA's is provided by a lattice calculation [44] which does not indicate any significant asymmetry. One may argue that the proton DA must be asymmetric to reflect the fact that the u quarks carry on average a larger fraction of the proton momentum than the d quarks. As shown in Ref. [45], to accomodate this observation one needs only a moderate shift of the DA maximum from the center point $x_1=x_2=x_3=1/3$. Such a shift does not produce a drastic enhancement of the hard contribution provided by the humpy DA's. However, with the asymptotic DA, the leading twist hard contribution completely fails to describe the data: it gives zero for the proton magnetic form

[4] See also the discussion in Sec. VI below.

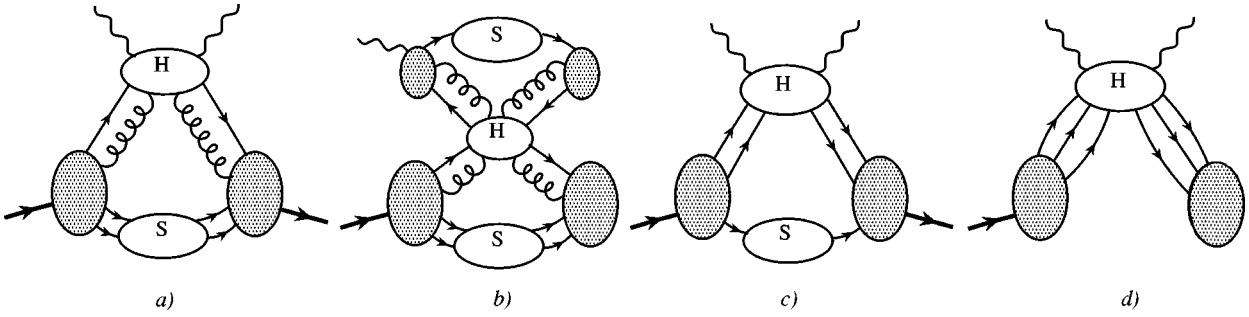

FIG. 4. Some configurations responsible for power-law asymptotic contributions for the WACS amplitude.

factor and a wrong-sign (positive) contribution for the neutron magnetic form factor, with the absolute magnitude of the latter being two orders of magnitude below the data [46].

Furthermore, as emphasized in Refs. [47,48], the whole strategy of getting enhancements from the humpy DA's is based on an implicit assumption that one may use the perturbative expressions $S(k)\sim\hat{k}/k^2$, $D(k)\sim 1/k^2$ for quark and gluon propagators up to very small virtualities $k^2 \lesssim (300\ \mathrm{MeV})^2$. It is worth recalling now why CZ-type DA's give an enhanced contribution. Since quarks in the proton carry only a fraction of the proton momentum, the characteristic virtualities $\sim x_i y_j t$ of ''hard'' quarks and gluons inside the short-distance subprocess are smaller than the total momentum transfer t. For a symmetric distribution, one would expect that $\langle x_i\rangle\sim 1/3$. With the humpy DA's, the average x_i for one of the u quarks is close to 1, and the dominant contribution comes from configurations in which this quark is active. Then fractions x_i related to passive quarks are rather small. It is precisely the small magnitude of the $\sim x_i y_j t$ denominators of quark and gluon propagators which produces the enhancement in the case of the CZ-type DA's. Hence, to get large hard contributions, it is absolutely necessary to assume that the perturbative expressions $S(k)\sim\hat{k}/k^2$, $D(k)\sim 1/k^2$ for quark and gluon propagators may be trusted up to very small virtualities.

An instructive illustration of possible modifications due to finite size or transverse momentum effects is given by the light-cone calculation of the $\gamma^*\gamma\pi^0$ amplitude [16,42] in which hard propagator of a *massless* quark is convoluted with the two-body wave function $\Psi(x,k_\perp)$. Assuming a Gaussian dependence $\Psi(x,k_\perp)\sim\exp[-k_\perp^2/2x\bar{x}\sigma]$ on transverse momentum, one can easily calculate the $k_\perp$ integral to see that the PQCD propagator factor $1/xQ^2$ is substituted by the combination $(1-\exp[-xQ^2/2\bar{x}\sigma])/xQ^2$ which monotonically tends to a finite limit $1/2\sigma$ as $x\to 0$. Hence, the effective virtuality is always larger than 2σ. The suppression of low virtualities has a simple explanation: propagation of quarks and gluons in the transverse direction is restricted by the finite size of the hadron. Numerically, $2\sigma\approx 1.35\ \mathrm{GeV}^2$ in that case. However, even a milder modification of the ''hard'' propagators by effective quark and gluon masses $1/k^2\to 1/(k^2-M^2)$ with $M^2\sim 0.1\ \mathrm{GeV}^2$ or model inclusion of transverse momentum effects strongly reduces the magnitude of hard contributions [49], especially when the CZ type DA's are used. For these reasons, a scenario with humpy DA's and bare $\sim 1/x_i y_j t$ propagators (which amounts to ignoring finite-size effects) considerably overestimates the size of hard contributions.

The relative smallness of hard contributions can be easily understood within the QCD sum rule context. The soft contribution is dual to the lowest-order diagram while the gluon exchange terms appear in diagrams having a higher order in α_s which results in the usual $\alpha_s/\pi\sim 1/10$ suppression factor per each extra loop. In particular, the α_s/π suppression factor is clearly visible in the expression for the hard contribution to the pion form factor [50–53]

$$F_\pi^{\mathrm{hard}}(Q^2)\big|_{\varphi_\pi=\varphi_\pi^{as}}=\frac{8\pi\alpha_s f_\pi^2}{Q^2}=2\left(\frac{\alpha_s}{\pi}\right)\frac{s_0}{Q^2}. \qquad (20)$$

Here, the combination $s_0=4\pi^2 f_\pi^2\approx 0.67\ \mathrm{GeV}^2\sim m_\rho^2$ is what is usually called the ''typical hadronic scale'' in the case of the pion. At asymptotically high Q^2, the $O(\alpha_s/\pi)$ suppression of the hard terms is more than compensated by their slower decrease with Q^2. However, such a compensation does not occur in the subasymptotic region where the soft contributions, as we have seen, may have the same effective power behavior as that predicted by the asymptotic quark counting rules for the hard contributions. In Ref. [54], both the soft contribution and the $O(\alpha_s)$ corrections for the pion form factor were calculated together within a QCD sum rule inspired approach. The ratio of the $O(\alpha_s)$ terms to the soft contribution was shown to be in full agreement with the expectation based on the α_s/π per loop suppression.

V. COMPTON SCATTERING AMPLITUDE AT LARGE MOMENTUM TRANSFER

With both photons real, it is not sufficient to have large photon energy to ensure short-distance dominance: the large-s, small-t region is strongly affected by Regge contributions. Hence, having large $|t|\gtrsim 1\ \mathrm{GeV}^2$ is a necessary condition for revealing short-distance dynamics.

Consider the Compton scattering amplitude for large values of s, u, and t. According to a general rule (see, e.g., Ref. [5], and references therein), to find possible mechanisms generating power-law contributions in the asymptotic limit $s\sim -u\sim -t\sim Q^2$ (Q here is just a characteristic scale), we should look for subgraphs whose contraction into point or removal from the diagram kills its dependence on large vari-

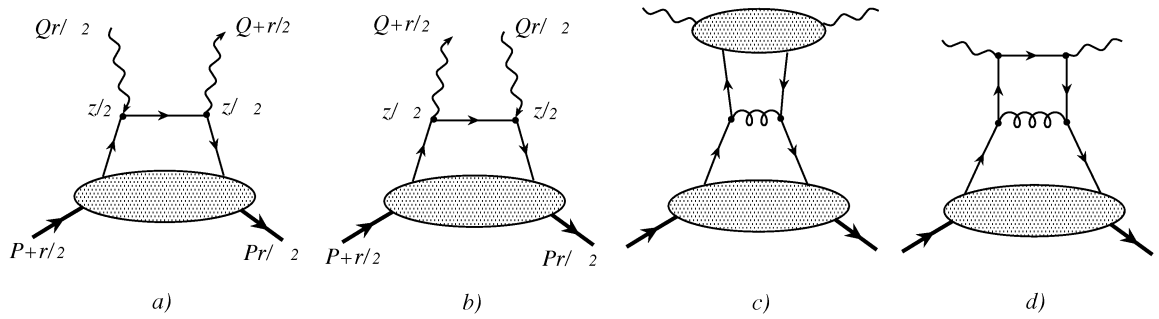

FIG. 5. Terms having $O(s^0)$ behavior for large s.

ables. Contracted subgraphs correspond to short-distance (SD) or hard regime while the removed ones to the infrared (IR) or soft regime. Some possibilities are shown in Fig. 4.

The power counting estimate for each SD subgraph is given by

$$A_H(Q) \sim Q^{4-N-\Sigma_i t_i}, \tag{21}$$

where N is the number of the external photon lines of the hard subgraph H and t_i is the twist of its ith external parton line ($t=1$ for quarks and physical gluons and $t=0$ for longitudinal gluons).

The perturbative estimate for an IR contribution is given by

$$A_S(Q) \lesssim Q^{-\Sigma_j t_j}, \tag{22}$$

where summation is over the external lines of the soft subgraph S. The infrared regime corresponds to the Feynman mechanism. However, we should keep in mind that the perturbative estimate implies a pointlike coupling of three quarks to the proton field while in real life the proton wave function is much softer. In particular, the perturbative estimate of the IR regime for the proton form factor gives $F(Q^2) \lesssim Q^{-4}$, allowing for $1/Q^4$ behavior in principle. To get such an asymptotic behavior from our ND models, we should assume that $f(x) \sim 1-x$ for x close to 1. More realistic functions dictate a faster decrease of $F(Q^2)$ in the asymptotic $Q \to \infty$ limit. This is not surprising as the IR regime is essentially nonperturbative and the Q dependence of the soft contributions should be better taken from a reasonable model rather than from perturbation theory. Again, since accessible Q's are far from being asymptotic, the ''observed'' power behavior of the soft contribution in this region may strongly differ from the asymptotic powers given by the Feynman mechanism.

The simplest contributions for the WACS amplitude are given by the s- and u-channel handbag diagrams, Fig. 5(a), 5(b). They correspond to a combined SD-IR regime of Fig. 4a: the dependence on s (or u) is killed by contracting into point the quark line connecting the photon vertices while the t dependence is killed by removal of a soft subgraph S. The SD regime in this case gives $A_H(s) \sim s^0$ behavior. The nonperturbative part is given by the proton nonforward DD's which determine the t dependence of the total contribution. Another $O(s^0)$ configuration is shown in Fig. 5(c). In this case, a hard gluon propagator is convoluted with the proton and photon DD's. Similarly to the usual photon structure functions, the photon DD's can be divided into the perturbative and the nonperturbative part. The latter corresponds to hadronic component of the real photon while the first one to a direct pointlike quark-photon coupling. It can be treated as a part of the one-loop correction to the handbag diagram [see Fig. 5(d)] and is accompanied by the α_s/π suppression factor. The hadronic component of the photon DD's has also an extra form factor type suppression $\sim m^2/t$.

Just like in the form factor case, the contribution dominating in the formal asymptotic limit $s, |t|, |u| \to \infty$, is given by diagrams corresponding to the pure SD regime, see Fig. 4(d). The hard subraph H involves two hard gluon exchanges which results in suppression by a factor $(\alpha_s/\pi)^2 \sim 1/100$ absent in the handbag term. The total contribution of all hard configurations was calculated by Farrar and Zhang [55] and then recalculated by Kronfeld and Nižić [56]. Again, a sufficiently large contribution is only obtained if one uses humpy DA's and $1/k^2$ propagators with no finite-size effects

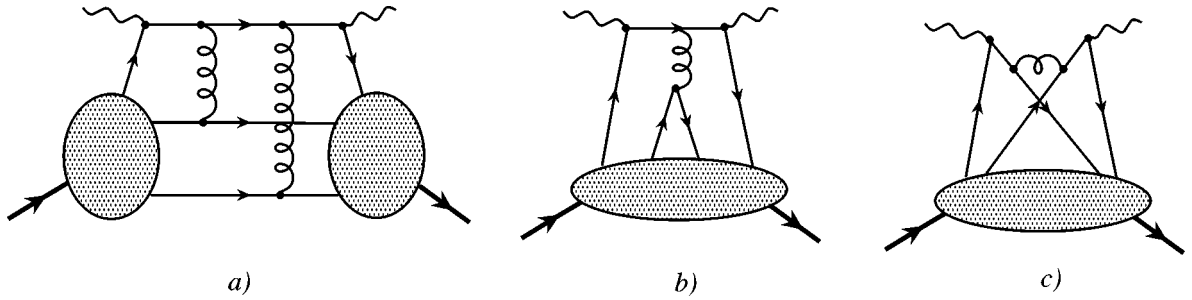

FIG. 6. Configurations involving double and single gluon exchange.

included. Even with such propagators, the WACS amplitude calculated assuming the asymptotic DA is negligibly small [57] compared to existing data. Our arguments concerning the reliability of CZ enhancements for form factors can be applied to the wide-angle Compton scattering without any changes. For these reasons, we ignore the hard contributions to the WACS amplitude as negligibly small.

Another type of configuration containing hard gluon exchange corresponds to the version of the combined SD-IR regime shown in Fig. 4(c). In particular, they include diagrams such as Fig. 6(b) and also diagrams with photons coupled to different quarks [''cat's ears,'' Fig. 6(c)]. Such contributions have both higher order and higher twist. This brings in the α_s/π factor and an extra $1/s$ suppression. The latter is partially compensated by a slower falloff of the four-quark DD's with t since only one valence quark should change its momentum.

VI. MODEL FOR WIDE-ANGLE COMPTON SCATTERING AMPLITUDE

In this paper, we neglect all the suppressed terms and deal only with the handbag contributions, Figs. 5(a), 5(b), in which the highly virtual quark propagator connecting the photon vertices is convoluted with nonforward proton DD's parametrizing the overlap of soft wave functions. Since the basic scale $4\lambda^2$ characterizing the t dependence of DD's in our model is 2.8 GeV^2, while existing data are all at momentum transfers t below 5 GeV^2, we deal with the region where the asymptotic estimate (Feynman mechanism) for the overlap contribution is not working yet. In the coordinate representation, the sum of two handbag contributions to the Compton amplitude can be written as

$$M^{\mu\nu}(p,p';q,q')=\sum_a e_a^2\int e^{-i(Qz)}\langle p'|[\bar{\psi}_a(z/2)\gamma^\mu S^c(z)\gamma^\nu\psi_a(-z/2)+\bar{\psi}_a(-z/2)\gamma^\nu S^c(-z)\gamma^\mu\psi_a(z/2)]|p\rangle d^4z, \quad (23)$$

where $Q=(q+q')/2$ and $S^c(z)=i\hat{z}/2\pi^2(z^2)^2$ is the hard quark propagator (throughout, we use the ''hat notation'' $\hat{z}\equiv z_\alpha\gamma^\alpha$). The summation over the twist-0 longitudinal gluons adds the usual gauge link between the $\bar{\psi}$, ψ fields which we do not write down explicitly [gauge link disappears, e.g., in the Fock-Schwinger gauge $z^\alpha A_\alpha(z)=0$]. Because of the symmetry of the problem, it is convenient to use $P=(p+p')/2$ (see Ref. [2]) and $r=p-p'$ as the basic momenta. Applying the Fiertz transformation and introducing the double distributions by

$$\langle p'|\bar{\psi}_a(-z/2)\hat{z}\psi_a(z/2)|p\rangle=\bar{u}(p')\hat{z}u(p)\int_0^1 dx\int_{-\bar{x}/2}^{\bar{x}/2}[e^{-i(kz)}\tilde{F}^a(x,\tilde{y};t)-e^{i(kz)}\tilde{F}^{\bar{a}}(x,\tilde{y};t)]d\tilde{y}$$

$$+\frac{1}{4m_p}\bar{u}(p')(\hat{z}\hat{r}-\hat{r}\hat{z})u(p)\int_0^1 dx\int_{-\bar{x}/2}^{\bar{x}/2}[e^{-i(kz)}\tilde{K}^a(x,\tilde{y};t)-e^{i(kz)}\tilde{K}^{\bar{a}}(x,\tilde{y};t)]d\tilde{y}+O(z^2)\ \text{terms} \quad (24)$$

(we use here the shorthand notation $k\equiv xP+\tilde{y}r$) and similarly for the parton helicity sensitive operators

$$\langle p'|\bar{\psi}_a(-z/2)\hat{z}\gamma_5\psi_a(z/2)|p\rangle=\bar{u}(p')\hat{z}\gamma_5u(p)\int_0^1 dx\int_{-\bar{x}/2}^{\bar{x}/2}[e^{-i(kz)}\tilde{G}^a(x,\tilde{y};t)+e^{i(kz)}\tilde{G}^{\bar{a}}(x,\tilde{y};t)]d\tilde{y}$$

$$+\frac{(rz)}{m_p}\bar{u}(p')\gamma_5u(p)\int_0^1 dx\int_{-\bar{x}/2}^{\bar{x}/2}[e^{-i(kz)}\tilde{P}^a(x,\tilde{y};t)+e^{i(kz)}\tilde{P}^{\bar{a}}(x,\tilde{y};t)]d\tilde{y}+O(z^2)\ \text{terms}, \quad (25)$$

we arrive at a leading-twist QCD parton picture with the tilded DD's serving as functions describing the long-distance dynamics. The new DD's $\tilde{F}^a(x,\tilde{y};t)$, etc., are related to the original DD's $F^a(x,y;t)$ discussed in Section II by the shift $y=\tilde{y}+\bar{x}/2$. Therefore, integrating $\tilde{F}(x,\tilde{y};t)$ over $\tilde{y}$ one obtains the same nonforward densities $\mathcal{F}(x;t)$. The hard quark propagators for the s and u channel handbag diagrams in this picture look similar to

$$\frac{x\hat{P}+\tilde{y}\hat{r}+\hat{Q}}{(xP+\tilde{y}r+Q)^2}=\frac{x\hat{P}+\tilde{y}\hat{r}+\hat{Q}}{x\tilde{s}-(\bar{x^2}/4-\tilde{y}^2)t+x^2m_p^2}$$

and

$$\frac{x\hat{P}+\tilde{y}\hat{r}-\hat{Q}}{(xP+\tilde{y}r-Q)^2}=\frac{x\hat{P}+\tilde{y}\hat{r}-\hat{Q}}{x\tilde{u}-(\bar{x^2}/4-\tilde{y}^2)t+x^2m_p^2}, \quad (26)$$

respectively. We denote $\tilde{s}=2(pq)=s-m^2$ and $\tilde{u}=-2(pq')=u-m^2$. Since DD's are even functions of $\tilde{y}$ [58], the $\tilde{y}\hat{r}$ terms in the numerators can be dropped. It is legitimate to keep $O(m_p^2)$ and $O(t)$ terms in the denominators: the dependence of hard propagators on target parameters m_p^2 and t can be calculated exactly because of the effect analogous to the ξ-scaling in DIS [9] (see also Ref. [36]). Note that the t correction to hard propagators disappears in the large-t limit dominated by the $x\sim 1$ integration. The t corrections are the

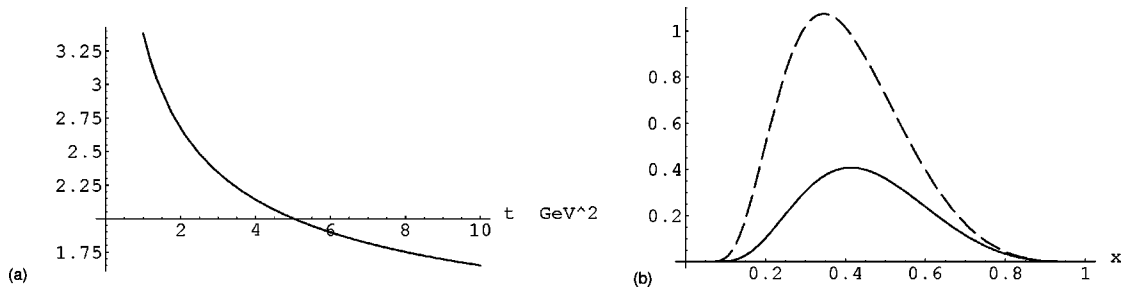

FIG. 7. (a) Ratio $R_1^u(t)/F_1^u(t)$ and (b) Functions $\mathcal{F}^u(x;t)$ (solid line) and $\mathcal{F}^u(x;t)/x$ (dashed line) at $t=-2.5$ GeV^2.

largest for $y=0$. At this value and for $x=1/2$ and $t=u$ (c.m. angle of 90°), the t term in the denominator of the most important second propagator is only 1/8 of the u term. This ratio increases to 1/3 for $x=1/3$. However, at nonzero $\tilde{y}$ values, the t corrections are smaller. Hence, the t corrections in the denominators of hard propagators can produce 10–20 % effects and should be included in a complete analysis. In the present paper, we consider a simplified approximation in which these terms are neglected and hard propagators are given by the $\tilde{y}$-independent expressions $(x\hat{P}+\hat{Q})/x\tilde{s}$ and $(x\hat{P}+\hat{Q})/x\tilde{u}$. As a result, the $\tilde{y}$ integration acts only on the DD's $\tilde{F}(x,\tilde{y};t)$ and converts them into nonforward densities $\mathcal{F}(x,t)$. The latter would appear then through two types of integrals

$$\int_0^1 \mathcal{F}^a(x,t)dx \equiv F_1^a(t) \quad \text{and} \quad \int_0^1 \mathcal{F}^a(x,t)\frac{dx}{x} \equiv R_1^a(t), \tag{27}$$

and similarly for $\mathcal{K},G,P$. The functions $F_1^a(t)$ are the flavor components of the usual $F_1(t)$ form factor while $R_1^a(t)$ are the flavor components of a new form factor specific to the wide-angle Compton scattering. In the formal asymptotic limit $|t|\to\infty$, the x integrals for $F_1^a(t)$ and $R_1^a(t)$ are both dominated in our model by the $x\sim 1$ region: the large-t behavior of these functions is governed by the Feynman mechanism and their ratio tends to 1 as $|t|$ increases [see Fig. 7(a)]. However, due to large value of the effective scale $4\lambda^2=2.8$ GeV^2, the accessible momentum transfers $t \lesssim 5$ GeV^2 are very far from being asymptotic.

In Fig. 7(b) we plot $\mathcal{F}^u(x;t)$ and $\mathcal{F}^u(x;t)/x$ at $t=-2.5$ GeV^2. It is clear that the relevant integrals are dominated by rather small x values $x\lesssim 0.5$ which results in a strong enhancement of $R_1^u(t)$ compared to $F_1^u(t)$ for $|t| \lesssim 5$ GeV^2. Note also that the $\langle p'|\cdots x\hat{P}\cdots|p\rangle$ matrix elements can produce only t as a large variable while $\langle p'|\cdots\hat{Q}\cdots|p\rangle$ gives s. As a result, the enhanced form factors $R_1^a(t)$ are accompanied by extra s/t enhancement factors compared to the $F_1^a(t)$ terms. In the cross section, these enhancements are squared, i.e., the contributions due to the nonenhanced form factors $F_1^a(t)$ are always accompanied by t^2/s^2 factors which are smaller than 1/4 for c.m. angles below 90°. Because of double suppression, we neglect $F_1^a(t)$ terms in the present simplified approach.

The contribution due to the $\mathcal{K}$ functions appears through the flavor components $F_2^a(t)$ of the $F_2(t)$ form factor and their enhanced analogues $R_2^a(t)$. The major part of contributions due to the $\mathcal{K}$-type ND's appears in the combination $R_1^2(t)-(t/4m_p^2)R_2^2(t)$. Experimentally, $F_2(t)/F_1(t) \approx 1$ GeV$^2/|t|$. Since $R_2/F_2 \sim R_1/F_1 \sim 1/\langle x\rangle$, $R_2(t)$ is similarly suppressed compared to $R_1(t)$, and we neglect contributions due to the $R_2^a(t)$ form factors. We also neglect here the terms with another spin-flip distribution $\mathcal{P}$ related to the pseudoscalar form factor $G_P(t)$ which is dominated by t-channel pion exchange. Our calculations show that the contribution due to the parton helicity sensitive densities $\mathcal{G}^a$ is suppressed by the factor $t^2/2s^2$ compared to that due to the $\mathcal{F}^a$ densities. This factor only reaches 1/8 for the c.m. angle of 90°, and hence the $\mathcal{G}^a$ contributions are not very significant numerically. For simplicity, we approximate $\mathcal{G}^a(x,t)$ by $\mathcal{F}^a(x,t)$. After all these approximations, the WACS cross section is given by the product

$$\frac{d\sigma}{dt} \approx \frac{2\pi\alpha^2}{\tilde{s}^2}\left[\frac{(pq)}{(pq')}+\frac{(pq')}{(pq)}\right]R_1^2(t), \tag{28}$$

of the Klein-Nishina cross section [in which we dropped $O(m^2)$ and $O(m^4)$ terms] and the square of the $R_1(t)$ form factor

$$R_1(t)=\sum_a e_a^2[R_1^a(t)+\bar{R}_1^a(t)]. \tag{29}$$

In our model, $R_1(t)$ is given by

$$R_1(t)=\int_0^1 [e_u^2 f_u^{\rm val}(x)+e_d^2 f_d^{\rm val}(x)+2(e_u^2+e_d^2+e_s^2)f^{\rm sea}(x)] \times e^{\bar{x}t/4x\lambda^2}\frac{dx}{x}. \tag{30}$$

We included here the sea distributions assuming that they are all equal $f^{\rm sea}(x)=f_{u,d,s}^{\rm sea}(x)=f_{\bar{u},\bar{d},\bar{s}}(x)$ and using a simplified parametrization

$$f^{\rm sea}(x)=0.5x^{-0.75}(1-x)^7 \tag{31}$$

which accurately reproduces the GRV formula for $Q^2 \sim 1$ GeV^2. Due to suppression of the small-x region by the

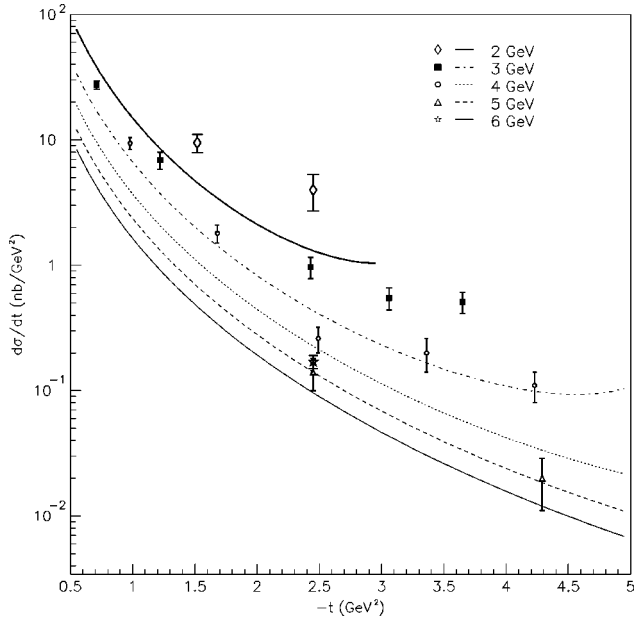

FIG. 8. WACS cross section versus t: comparison of results based on Eq. (28) with experimental data.

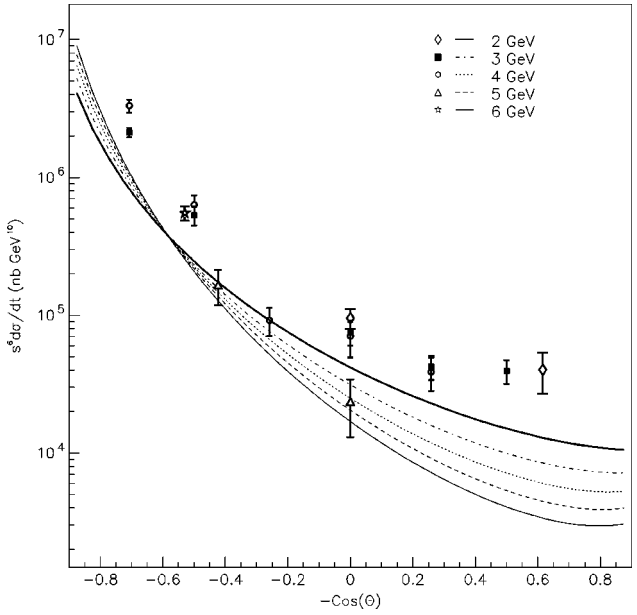

FIG. 9. Angular dependence of the combination $s^6(d\sigma/dt)$.

exponential $\exp[\overline{xt}/4x\lambda^2]$, the sea quark contribution is rather small ($\sim 10\%$) even for $-t\sim 1$ GeV^2 and is invisible for $-t\gtrsim 3$ GeV^2.

Comparison with existing data [59] is shown in Fig. 8. Our curves follow the data pattern but are systematically lower by a factor of 2, with disagreement becoming more pronounced as the scattering angle increases. Since we neglected several terms each capable of producing up to a 20% correction in the amplitude, we consider the agreement between our curves and the data as encouraging. The most important corrections which should be included in a more detailed investigation are the t corrections in the denominators of hard propagators and contributions due to the ''nonleading'' $\mathcal{K},G,P$ nonforward densities. The latter, as noted above, are usually accompanied by t/s and t/u factors, i.e., their contribution becomes more significant at larger angles. The t correction in the most important hard propagator term $1/[x\tilde{u}-(\overline{x^2}/4-\tilde{y}^2)t+x^2m_p^2]$ also enhances the amplitude at large angles.

The angular dependence of our results for the combination $s^6(d\sigma/dt)$ is shown in Fig. 9. All the curves for initial photon ehergies 2, 3, 4, 5, and 6 GeV intersect each other at $\theta_{\text{c.m.}}\sim 60°$. This is in good agreement with experimental data of Ref. [59] where the differential cross section at fixed cm angles was fitted by powers of s: $d\sigma/dt\sim s^{-n(\theta)}$ with $n^{\text{exp}}(60°)=5.9\pm 0.3$. Our curves (see Fig. 10) correspond to $n^{\text{soft}}(60°)\approx 6.1$ and $n^{\text{soft}}(90°)\approx 6.7$ which also agrees with the experimental result $n^{\text{exp}}(90°)=7.1\pm 0.4$.

This can be compared with the scaling behavior of the asymptotic hard contribution: modulo logarithms contained in the α_s factors, they have a universal angle-independent power $n^{\text{hard}}(\theta)=6$. For $\theta_{\text{c.m.}}=105°$, the experimental result based on just two data points is $n^{\text{exp}}(105°)=6.2\pm 1.4$, while our model gives $n^{\text{soft}}(105°)\approx 7.0$. Clearly, better data are needed to draw any conclusions here.

VII. SUMMARY AND CONCLUSIONS

In this paper, we introduced nonforward parton densities $\mathcal{F}(x;t)$ which are the simplest hybrids of the usual parton densities and hadronic form factors. We proposed a simple model for the quark ND's $\mathcal{F}^a(x;t)$ which, in the $t\to 0$ limit, reproduces the standard parametrizations for the usual parton densities and gives a reasonable description of existing data on the $F_1^p(t)$ form factor in a wide range 1 GeV$^2\lesssim -t \lesssim 10$ GeV^2 of momentum transfer. The crucial observation is that though our model includes only the soft contribution, the form factor is dominated at accessible energies by rather

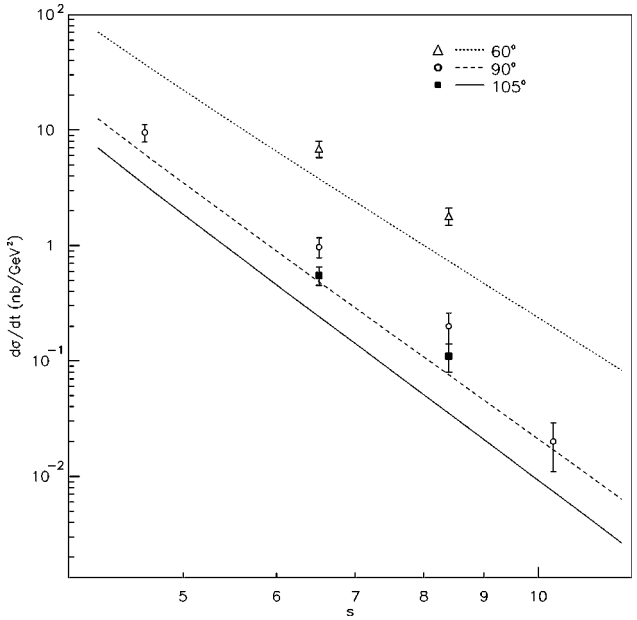

FIG. 10. s dependence of the differential cross section $d\sigma/dt$ for $\theta=60°$ (dotted line), $\theta=90°$ (dashed line), and $\theta=105°$ (solid line).

small momentum fractions $x \sim 0.5$ and asymptotic estimates for soft contributions (corresponding to Feynman mechanism, i.e., dominance of the $x \sim 1$ region) are not working yet. We gave arguments that the wide-angle Compton scattering amplitude in the same t region is dominated by two handbag diagrams. We also found that the largest term contains the same ND's $\mathcal{F}(x;t)$ which determine the behavior of $F_1^p(t)$. However, due to the extra $1/x$ factor and small value of $\langle x \rangle$, the WACS amplitude gets a strong enhancement bringing our predictions close to existing experimental data. Still, there remains a systematic difference by a factor of 2 between our results and the data.

On the experimental side, data of higher quality are needed. They are expected from a future experiment at Jefferson Lab [60], in which better statistical accuracy is expected and several new ideas will be used to control the systematic errors.

On the theoretical side, a more detailed approach is needed which would take into account all nonforward densities. A more complete analysis should also include calculable t and m_p^2 dependences of the hard quark propagators and terms which are not enhanced by the $1/\langle x \rangle$ factors. It should be emphasized that keeping the t terms in the denominators of hard propagators requires a major change in the whole approach: it would be no longer possible to get a simplified description in terms of the nonforward densities $\mathcal{F}(x;t)$. One should deal then with double distributions $\tilde{F}(x,\tilde{y};t)$ in all their complexity and construct a model for their profile in the $\tilde{y}$ direction. This observation also demonstrates that the double distributions $F(x,y;t)$ are the primary objects for analyzing nonforward matrix elements of light cone operators. They are more fundamental than their reductions such as nonforward, off-forward, etc., distributions which work only when the hard part of the relevant amplitude depends on a particular linear combination $x+y\zeta$ of its two arguments x and y. A more detailed discussion of double distributions will be given in a forthcoming publication [61].

ACKNOWLEDGMENTS

This investigation was strongly influenced by the real Compton scattering enthusiasts C. E. Hyde-Wright, A. Nathan, and B. Wojtsekhowski, to whom I am most grateful for numerous discussions. I also benefited from discussions and communications with A. Afanasev, I. Balitsky, S. Brodsky, C. Coriano, N. Isgur, and I. Musatov. I am especially grateful to I. Musatov for help with figures and for patiently teaching me how to use his FEYNMAN GRAPH program [62]. This work was supported by the U.S. Department of Energy under Contract No. DE-AC05-84ER40150.

[1] R. P. Feynman, *The Photon-Hadron Interaction* (Benjamin, Reading, 1972).
[2] X. Ji, Phys. Rev. Lett. **78**, 610 (1997).
[3] A. V. Radyushkin, Phys. Lett. B **380**, 417 (1996).
[4] X. Ji, Phys. Rev. D **55**, 7114 (1997).
[5] A. V. Radyushkin, Phys. Rev. D **56**, 5524 (1997).
[6] X. Ji and J. Osborne, hep-ph/9801260.
[7] J. C. Collins and A. Freund, hep-ph/9801262.
[8] O. Nachtmann, Nucl. Phys. **B63**, 237 (1973).
[9] H. Georgi and H. D. Politzer, Phys. Rev. D **14**, 1829 (1976).
[10] A. V. Radyushkin, Phys. Lett. B **385**, 333 (1996).
[11] J. C. Collins, L. Frankfurt, and M. Strikman, Phys. Rev. D **56**, 2982 (1997).
[12] M. Diehl, T. Gousset, B. Pire, and J. Ralston, Phys. Lett. B **411**, 193 (1997).
[13] A. D. Martin and M. G. Ryskin, Phys. Rev. D **57**, 6692 (1998).
[14] I. I. Balitsky and A. V. Radyushkin, Phys. Lett. B **413**, 114 (1997).
[15] J. Blumlein, B. Geyer, and D. Robaschik, Phys. Lett. B **406**, 161 (1997).
[16] S. J. Brodsky, T. Huang, and G. P. Lepage, in *Particles and Fields 2*, Proceedings of the Banff Summer Institute, Banff, Alberta, 1981, edited by A. Z. Capri and A. N. Kamal (Plenum, New York, 1983), p. 143.
[17] M. Gluck, E. Reya, and A. Vogt, Z. Phys. C **67**, 433 (1995).
[18] L. Andivahis *et al.*, Phys. Rev. D **50**, 5491 (1994).
[19] B. L. Ioffe and A. V. Smilga, Nucl. Phys. **B232**, 109 (1984).
[20] I. I. Balitsky and A. V. Yung, Phys. Lett. **129B**, 328 (1983).
[21] V. A. Nesterenko and A. V. Radyushkin, JETP Lett. **39**, 707 (1984).
[22] V. M. Belyaev and Ya. I. Kogan, Int. J. Mod. Phys. A **8**, 153 (1993).
[23] I. I. Balitsky, Phys. Lett. **114B**, 53 (1982).
[24] S. J. Brodsky and G. R. Farrar, Phys. Rev. Lett. **31**, 1153 (1973).
[25] V. A. Matveev, R. M. Muradyan, and A. N. Tavkhelidze, Lett. Nuovo Cimento **7**, 719 (1973).
[26] G. P. Lepage and S. J. Brodsky, Phys. Rev. Lett. **43**, 545 (1979); **43**, 1625 (1979).
[27] V. L. Chernyak and A. R. Zhitnitskyo, Phys. Rep. **112**, 173 (1984).
[28] V. L. Chernyak and I. R. Zhitnitsky, Nucl. Phys. **B246**, 52 (1984).
[29] S. V. Mikhailov and A. V. Radyushkin, JETP Lett. **43**, 712 (1986); Sov. J. Nucl. Phys. **49**, 494 (1989).
[30] S. V. Mikhailov and A. V. Radyushkin, Phys. Rev. D **45**, 1754 (1992).
[31] D. Daniel, R. Gupta, and D. G. Richards, Phys. Rev. D **43**, 3715 (1991).
[32] V. M. Braun and I. Filyanov, Z. Phys. C **44**, 157 (1989).
[33] A. V. Radyushkin, in *Continuous Advances in QCD*, Proceedings of the Workshop, Minneapolis, Minnesota, 1994, edited by A. V. Smilga (World Scientific, Singapore, 1994), p. 238; hep-ph/9406237.
[34] A. P. Bakulev and S. V. Mikhailov, Z. Phys. C **65**, 451 (1995).
[35] V. Yu. Petrov and P. V. Pobylitsa, hep-ph/9712203.
[36] A. V. Radyushkin and R. Ruskov, Nucl. Phys. **B481**, 625 (1996).
[37] V. M. Belyaev and M. B. Johnson, Phys. Rev. D **56**, 1481 (1997).

[38] V. M. Belyaev and M. B. Johnson, hep-ph/9703244.
[39] V. L. Chernyak and A. R. Zhitnitsky, Nucl. Phys. **B201**, 492 (1984); **B214**, 547(E) (1984).
[40] CLEO Collaboration, J. Gronberg *et al.*, Phys. Rev. D **57**, 33 (1998).
[41] E. Braaten, Phys. Rev. D **28**, 524 (1983).
[42] I. V. Musatov and A. V. Radyushkin, Phys. Rev. D **56**, 2713 (1997).
[43] S. J. Brodsky, C.-R. Ji, A. Pang, and D. G. Robertson, Phys. Rev. D **57**, 245 (1998).
[44] G. Martinelli and C. T. Sachrajda, Phys. Lett. B **217**, 319 (1989).
[45] J. Bolz and P. Kroll, Z. Phys. A **356**, 327 (1996).
[46] V. M. Belyaev and B. L. Ioffe, Sov. Phys. JETP **56**, 493 (1982).
[47] N. Isgur and C. H. Llewellyn Smith, Nucl. Phys. **B317**, 526 (1989).
[48] A. V. Radyushkin, Nucl. Phys. **A532**, 141 (1991).
[49] J. Bolz *et al.*, Z. Phys. C **66**, 267 (1995).
[50] V. L. Chernyak, A. R. Zhitnitsky, and V. G. Serbo, JETP Lett. **26**, 594 (1977).
[51] G. R. Farrar and D. R. Jackson, Phys. Rev. Lett. **43**, 246 (1979).
[52] A. V. Efremov and A. V. Radyushkin, Phys. Lett. **94B**, 245 (1980).
[53] G. P. Lepage and S. J. Brodsky, Phys. Lett. **87B**, 359 (1979).
[54] A. Szczepaniak, C.-R. Ji, and A. Radyushkin, Phys. Rev. D **57**, 2813 (1998).
[55] G. R. Farrar and H. Zhang, Phys. Rev. D **41**, 3348 (1990); **42**, 2413(E) (1990).
[56] A. Kronfeld and B. Nižić, Phys. Rev. D **44**, 3445 (1991); **46**, 2272(E) (1992).
[57] M. Vanderhaeghen, Report No. DAPNIA-SPHN-97-42, Saclay, 1997.
[58] L. Mankiewicz, G. Piller, and T. Weigl, hep-ph/9711227.
[59] M. A. Shupe *et al.*, Phys. Rev. D **19**, 1921 (1979).
[60] Jefferson Lab Hall A experiment No. 97-108.
[61] A. V. Radyushkin, Report No. JLAB-THY-98-16 (1998); hep-ph/9805342.
[62] I. V. Musatov, FEYNMAN GRAPH, program available at URL http://www.physics.odu.edu/~musatov/FG/.